

# Formation and Dissolution of Gold Nanocrystal Superlattices in a Colloidal Solution

X. M. Lin, G. M. Wang, and C. M. Sorensen\*

Condensed Matter Laboratory, Department of Physics, Kansas State University, Manhattan, Kansas 66506

K. J. Klabunde

Department of Chemistry, Kansas State University, Manhattan, Kansas 66506

Received: March 2, 1999; In Final Form: April 19, 1999

Gold nanocrystal superlattices were synthesized in colloidal form by ligating the nanocrystal surface with dodecanethiol ligand. Formation and dissolution of the superlattices in the colloid were studied by UV–vis spectroscopy and dynamic light scattering. The phase boundary between nanocrystals and their superlattices in solution was found to be similar to the case of macroscopic crystals made of atoms or molecules. Lowering the temperature across the phase boundary resulted in nucleation of nanocrystals into superlattices and the superlattice size depended on the rate of nucleation. UV–vis spectroscopy and dynamic light scattering also showed that thermal dissolution of the superlattices occurred after the temperature of the colloid was raised across the phase boundary.

## I. Introduction

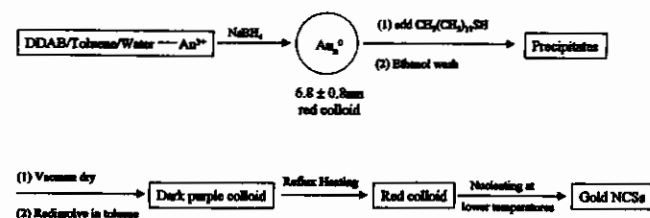
During the past decade, nanocrystal research has been focused on two major properties of finite size materials, namely, quantum size effects and surface/interface effects.<sup>1</sup> A new trend, however, has emerged in the past few years to arrange the nanocrystals into two or three dimensional superlattices.<sup>2,3</sup> The ability to synthesize nanocrystal superlattice (NCS) structures will provide a new horizon to study the collective properties due to the particle interaction and develop future optical<sup>4</sup> and information storage devices.<sup>5</sup> Several groups are striving to control nanocrystal size through size selective precipitation methods and create NCSs through evaporation of colloids containing lyophobic nanocrystals on a substrate. Face-center-cubic CdSe NCSs were synthesized through reducing the solubility of particles by slowly evaporating one component of a solvent mixture.<sup>6</sup> Oxide,<sup>7</sup> sulfide,<sup>8</sup> and noble metal<sup>9,10</sup> NCSs were spontaneously formed by evaporating the solvent. Kogel et al.<sup>9</sup> and Ohara et al.<sup>11</sup> showed that, unlike micron size hard spheres, self-organization of nanocrystals on a substrate is not simply entropy driven. Instead, interactions between particles and between particle and substrate also play an important role in determining the packing morphology of the superlattices. Linking molecules have also been used to form two-dimensional gold NCSs.<sup>12</sup> Narrow size latex particles and nanometer ferritin molecules were self-assembled in thin liquid films with thickness comparable to the size of the particles.<sup>13</sup> All these methods of forming NCSs rely on modifying the nature of the nanocrystal surface and its surrounding environment and therefore control the interaction between different particles. Other physical methods such as electrophoretic deposition were also explored to form NCSs.<sup>14</sup> Recently, Whetten et al.<sup>15</sup> used a fractional crystallization technique to create gold and silver nanoparticles with a very narrow size distribution and NCSs with different structures were formed spontaneously after evaporating the solvent. Despite all these developments in recent years, most of the work has involved formation of two dimensional ordered films on a substrate by evaporation of the solvent, and there are only a couple of reports on three-dimensional superlattice formation.<sup>6,16</sup>

Forming bulk quantities of three-dimensional NCSs directly in a colloidal state still remains a challenge. We reported recently a simple method to induce superlattice formation directly in a slightly polydispersed gold colloid by modifying the nanocrystal surface with certain ligands.<sup>17</sup> In this paper, the formation and thermal dissolution of gold nanocrystal superlattices are studied. Transmission electron microscopy (TEM) and dynamic light scattering (DLS), also known as photon correlation spectroscopy (PCS), were used to show the existence of tertiary structures, namely single nanocrystals, superlattices and superlattice aggregates in the colloid. We show that the formation of NCSs from nanocrystal colloid resembles the formation of normal molecular crystals from a saturated solution. The thermal dissolution of the superlattices in the solvent was studied by both UV–vis spectroscopy and DLS.

## II. Sample Preparation

The synthetic procedure for gold NCSs was similar to the previously reported process.<sup>17</sup> Didodecyltrimethylammonium bromide (DDAB) was purchased from Fluka and used as received. Sodium borohydride, dodecanethiol, and gold chloride (99.99%) was obtained from Aldrich and used as received. Toluene was purchased from Fisher and was further purified by distillation. Deionized distilled water was obtained from a Barnstead nanopure system. Toluene and distilled water were first degassed by bubbling with dry argon gas for 2 h prior to the experiment. The degassing process is a necessary step for a well controlled growth of nanoparticles as pointed out by Wilcoxon et al.<sup>18</sup> All the synthetic steps were carried out in a dry Argon environment in order to prevent chemicals from absorbing moisture. A typical synthesis is given as follows (Scheme 1). DDAB (0.75 g) was dissolved in 5.2 mL of toluene to form a 0.35 M micelle solution. Gold chloride (15 mg) was then dissolved in 5 mL of the micelle solution by sonication to form a dark orange colored solution. Aqueous NaBH<sub>4</sub> solution (17  $\mu$ L 9.4 M) ([BH<sub>4</sub><sup>-</sup>]:[Au<sup>3+</sup>] = 3:1) was added while vigorously stirring the solution. The solution first decolorized and then turned to red after about 20 s. The mixture was stirred for

## SCHEME 1



15 min to ensure a complete reaction. TEM showed that the as prepared colloid contained 6.8 nm particles with a standard deviation of 0.8 nm. The gold colloid was then split into 1 mL portions in separate vials. Dodecanethiol (0.838 mL) was added as a ligand to each vial so that [ligand]:[DDAB] = 10:1. The solution was stirred for several minutes, 8 mL of ethanol was added to the vial and the solution was stirred for another several minutes. All the samples were left on the bench top overnight. Particle aggregates caused by the ethanol wash settled down to the bottom of the vial, leaving extra surfactant and reaction side products in the top supernatant layer. The top supernatant layer was then decanted from each vial. After the bottom precipitates were dried in vacuum, different amounts of toluene were added to each sample to form various concentrations of a bluish colloid. A brief reflux heating turned the color of the colloid from bluish to red: this indicated the aggregates were broken into single particles by heating. The red colloids were immediately transferred to heat baths set at different temperatures (ranging from 23 to 80 °C) and left undisturbed for a couple of days.

## III. Instrumental Methods

The size and the morphology of gold NCSs were examined using a Philips EM200 microscope. Nanosize gold colloids have a strong absorption in the visible range due to the surface plasmon absorption. The absorption peak position depends on the size, the coating environment, and the aggregation of the particles.<sup>19</sup> Milton Roy 3000 array spectrophotometer was used to measure the absorption of the colloids and thereby determine the state of aggregation.

Another method we applied to study the colloids was dynamic light scattering (DLS), also known as photon correlation spectroscopy (PCS). DLS measures the autocorrelation function  $C(t)$  of the intensity of the scattering light.<sup>20</sup>  $C(t)$  is defined as

$$C(t) = \langle I(0)I(t) \rangle \quad (1)$$

where  $I(t)$  is the scattering intensity at time  $t$ .  $\langle \dots \rangle$  indicates averaging over the measuring time. For monodispersed particles,  $C(t)$  is an exponential decay function.

$$C(t) = B + Ae^{-t/\tau_c} \quad (2)$$

where  $B = \langle I \rangle^2$  is the background or noise level,  $A = \langle I^2 \rangle - \langle I \rangle^2$  is the signal magnitude, and  $\tau_c$  is the correlation time. Assuming spherical particles, the correlation time is related to the size of particle by

$$\tau_c = \left( \frac{3\pi\eta d}{2k_B T q^2} \right) \quad (3)$$

where  $\eta$  is the viscosity of the solvent,  $d$  is the average diameter of the particles,  $k_B$  is the Boltzmann constant,  $T$  is the temperature of the colloid, and  $q$  is the magnitude of the scattering wave vector. By measuring the autocorrelation function  $C(t)$  and fitting it with (2), the correlation time, and

consequently, the particle size can be found. However, the measurements of a colloidal system can sometimes be complicated by several other factors. For our gold colloids, two major problems have to be addressed before reasonable information can be derived from these measurements. First, the single-exponential decay function for the correlation only applies to colloids with monodispersed particles. For colloids containing binary or tertiary structures with different sizes, extra exponential terms must be introduced. For example, a colloid that has tertiary structures must use the following fitting function:

$$C(t) = B + A_1 e^{-t/\tau_{c1}} + A_2 e^{-t/\tau_{c2}} + A_3 e^{-t/\tau_{c3}} \quad (4)$$

where each exponential term corresponds to one component of the tertiary structures. The scattering of light from colloidal particles scales as the sixth power of their size if their size is much smaller than the wavelength  $\lambda$ . Therefore, the coefficients  $A_i$  ( $i = 1, 2, 3$ ) in (4) rely heavily on the size and the concentration of each component. In some cases, one or two terms in the above equation might be dominant and the contribution from the others can be neglected. Secondly, strong absorption of some highly concentrated colloids induces local heating in the path of the laser beam, which in turn causes a change of optical index of refraction of the medium and a divergence of the beam. This phenomenon, normally called thermal blooming or the thermal lensing effect,<sup>21</sup> results in a faster decay of the correlation function than the exponential decay. A second cumulant term must be introduced in order to obtain the correct particle size from  $\tau_c$ .<sup>22</sup> The correlation function for a strongly absorbing monodispersed colloid therefore is

$$C(t) = B + Ae^{-t/\tau_c - t^2/\tau_t^2} \quad (5)$$

where the second cumulant  $\tau_t$  depends on the intensity of the incident beam and the properties of the absorbing medium.

## IV. Results

In our experiment, dodecanethiol ligand was used to modify the surface of the gold nanocrystals. The change of electron density on the particle surface and the change of adjacent environment by the ligand increase the attractive interaction between nanocrystals. As a comparison, unligated nanocrystals remained well dispersed in the colloid due to the strong electrostatic and steric repulsive interaction in the inverse micelle medium.

After they were reflux heated in the presence of dodecanethiol, all the samples kept at temperatures higher than 80 °C showed no sign of superlattice or other types of aggregate formation, because the increase of the free energy due to the ordering (entropy loss) is much larger than the lowering of the free energy from bringing particles into close contact. On the other hand, samples kept at temperatures lower than a certain critical temperature became supersaturated and nucleated into aggregates that have superlattice structures. The critical temperature depended on the concentration of the colloid. Figure 1 shows the TEM image of one of the superlattices formed at 60 °C in a colloid with gold nanocrystal concentration of  $0.24 \times 10^{-6}$  M. The picture was slightly underexposed because of the thermal instability of the lattice under the high intensity electron beam. However, the lattice fringes caused by the long range ordering of nanocrystals can be clearly identified, especially at the edge of the superlattice. These NCSs gradually aggregated together to form fractal-like aggregates and settled down to the bottom of the vial.



Figure 1. TEM image of gold nanocrystal superlattice formed from  $0.24 \times 10^{-6}$  M colloid at 60 °C.

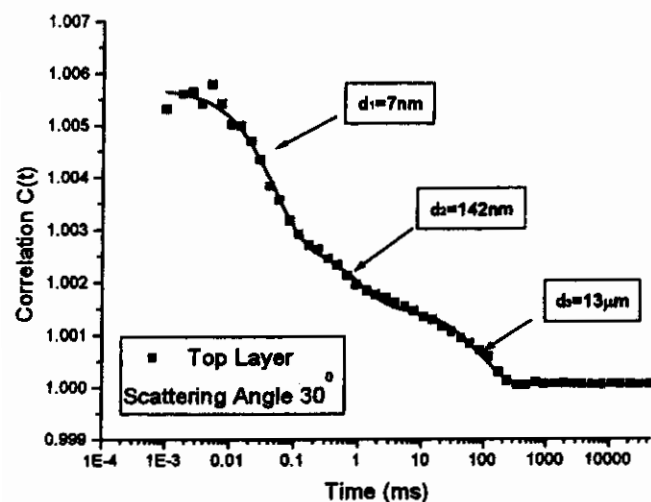


Figure 2. Correlation function  $C(t)$  measured by DLS on the top layer of the  $0.24 \times 10^{-6}$  M gold NCS colloid. Square dots are experimental data; solid line is fitting curve using (4).

The top layer of the samples that contained NCSs appeared red after being left undisturbed for a couple of days. TEM showed that this top layer contained mainly single nanocrystals. Figure 2 shows the DLS correlation function  $C(t)$  of the top layer of the  $0.24 \times 10^{-6}$  M colloid held at 23 °C. Three decays at different time ranges indicate the existence of tertiary structures in the colloid, namely, single nanocrystals, superlattices, and superlattice aggregates. Fitting these data with the function of three exponential decay terms (4) gives the corresponding sizes of 7 nm, 142 nm, and 13  $\mu$ m. These fitting results compare well with the direct TEM measurements on the same sample. The appearance of all three decays in the correlation function is due to the fact that the amount of superlattices and their aggregates was very small in the top layer of the colloid. The scattering from these large structures was comparable with the scattering from the large quantity of single nanocrystals. Moreover, the correlation decay times of all these structures occur at different times which are more than an order of magnitude apart.

Figure 3 shows the correlation function of the bottom layer of the same colloid. Different from the top layer, only the decays due to superlattices and their aggregates are visible (square dots

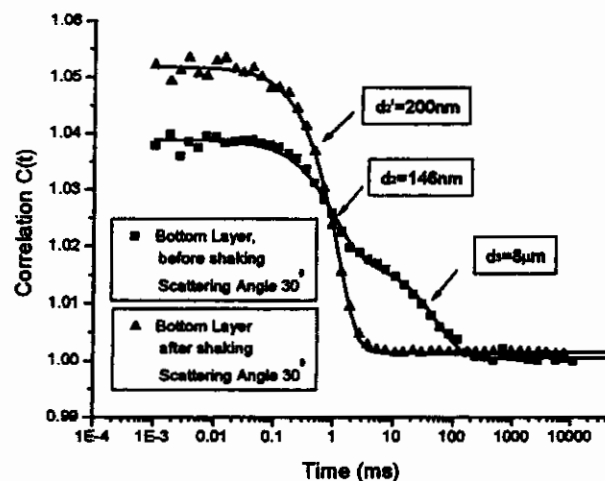


Figure 3. Correlation function  $C(t)$  measured by DLS on the bottom layer of the  $0.24 \times 10^{-6}$  M gold NCS colloid. Square dots are experimental data on the undisturbed sample; triangular dots are experimental data on the sample after being shaken. Solid lines are fitting curves using the two exponent decay function and (5) to account for thermal blooming.

TABLE 1: Phase Diagram of a Colloid Containing Gold Nanocrystals and Nanocrystal Superlattices

temperature (°C)	nanocrystal concentration ( $10^{-6}$ M)				
	0.06	0.10	0.15	0.24	0.40
80	red	red	red	red	red
60	red	red	red/purple	red/purple	red/purple
40	red	purple	purple	purple	purple
23	purple	purple	purple	purple	purple

in Figure 3). The decay from the single nanocrystals was not seen because it was overwhelmed by the scattering from superlattices and their aggregates. The aggregates of superlattices were only loosely bonded. This can be seen by simply shaking the colloid. The correlation function of the colloid after being shaken (triangle dots) showed only a single decay corresponding to the superlattice structures. In this case we fit the data with a two-cumulant decay function (5) because of the strong thermal blooming effect after the sample was shaken.

The formation of gold NCSs from colloidal nucleation resembles the formation of molecular crystals from a saturated solution. The nucleation process of NCSs depends on both the concentration and the temperature of the single-nanocrystal colloid. Samples synthesized with different gold concentrations were compared at different temperatures. Colloids containing NCSs appear to be purple and colloids without NCSs formation are red. Table 1 shows the results of visual inspection of these samples. A phase boundary between single-nanocrystal colloids and NCS colloids clearly exists. Figure 4 shows the TEM image of the superlattice structures nucleating at 23 and 60 °C from  $0.24 \times 10^{-6}$  M colloids. Superlattices formed at 60 °C were roughly 3 times the size of the superlattices formed at 23 °C. We believe that the difference in superlattice size was caused by the formation of a different amount of nucleation sites when the reflux heated samples were cooled to the two temperatures. For  $0.24 \times 10^{-6}$  M colloids, 60 °C is only slightly below the phase boundary; therefore, colloids quenched to this temperature had fewer nucleation sites and each nucleation site subsequently grew into a large size of superlattice. In comparison, colloids quickly quenched to 23 °C resulted in large number of nucleation sites and the simultaneous growing of all these sites result in smaller size of superlattices. DLS study of these colloids showed qualitatively the same results. Figure 5 is the correlation function of the bottom layer colloids (after being shaken)

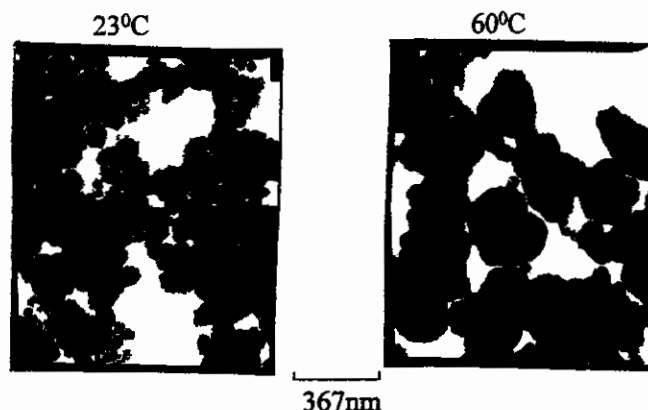


Figure 4. Gold NCSs formed from a  $0.24 \times 10^{-6}$  M colloid at different temperatures. (a) Formed at 23 °C. (b) Formed at 60 °C. (Note: heart-shaped particle in center is same as that in Figure 1.)

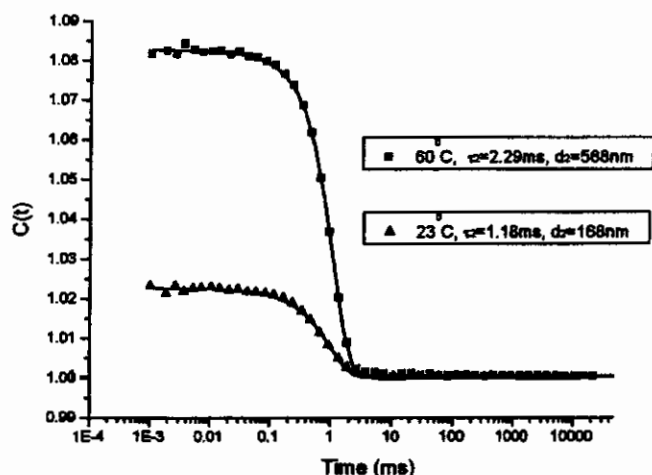


Figure 5. Correlation function  $C(t)$  measured by DLS on the  $0.24 \times 10^{-6}$  M NCS colloids formed at 23 and 60 °C.

measured for both the 60 and the 23 °C samples. After taking into account the temperature dependence of the solvent viscosity, the size of superlattices formed at 60 °C is roughly 3 times the size of the superlattices formed at 23 °C.

The formation of micron size particles in an ordered array has been known for a long time.<sup>23</sup> It relies on the balance between the long range van der Waals interaction, sometimes called the Hamaker interaction, and the repulsive electrostatic and steric interactions.<sup>24</sup> These interactions are described in detail by the DLVO theory,<sup>25</sup> which predicts a second minimum, usually beyond 3 nm from the primary energy barrier. The micron size colloidal particles can be relatively stable when they reside in this second minimum well.<sup>26</sup> The formation of nanocrystal superlattices from the colloid, on the other hand, requires a much more delicate balance between the attractive force and the repulsive interaction. This is due to the fact that nanocrystals have a much smaller second minimum in the potential curve as compared with micron size particles.<sup>2</sup> For the same reason, these superlattices can be easily dissolved upon heating the colloid. We can study the dissolution process by watching the optical properties of the NCS colloids. At room temperature, the colloids containing NCSs appeared purple, with a broad absorption band extended to the long wavelength of the visible region (top line in Figure 6). As the sample was heated, it crossed the phase boundary and the color of the colloid gradually changed to red, with the absorption spectra eventually changed to the single nanocrystal surface plasmon absorption at around 530 nm (bottom line in Figure 6). The change of

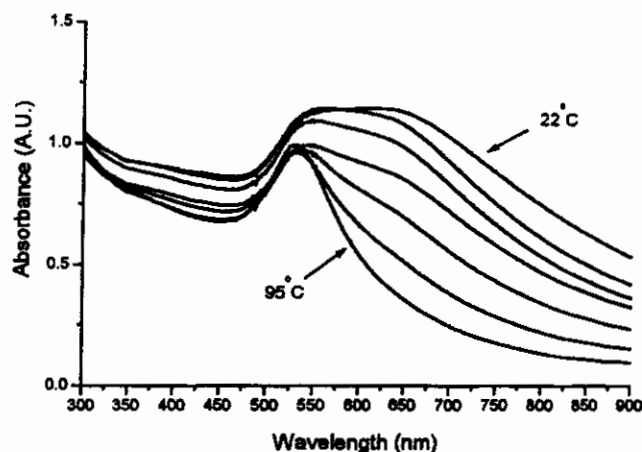


Figure 6. Change of UV-vis absorption curve of a NCS colloid as it was heated from 22 to 95 °C.

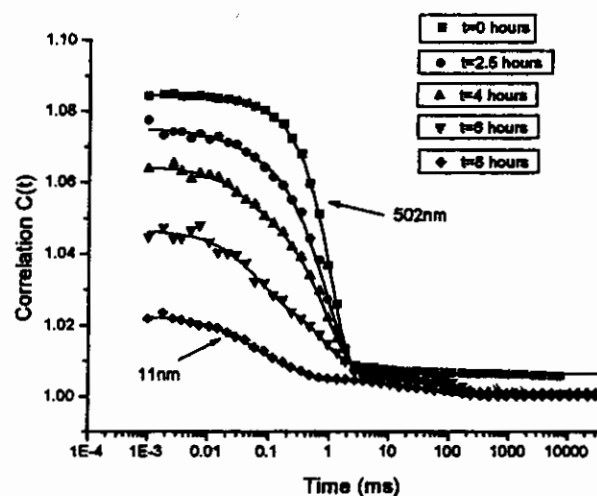


Figure 7. Time evolution of the correlation function  $C(t)$  of a  $0.15 \times 10^{-6}$  M NCS colloid maintained at 80 °C.

absorption spectra occurs within roughly 10 min. Dissolution of gold NCSs was also studied by DLS. A NCS colloid prepared at 23 °C with a concentration of  $0.15 \times 10^{-6}$  M was transferred into a heat bath at 80 °C. Figure 7 shows the time evolution of the correlation function of this colloid. The decay function at time  $t = 0$  corresponds to a size of 502 nm, larger than the size we have observed in TEM (around 250 nm). This is probably due to initial slight aggregation of superlattices. After about 8 h, the correlation function is dominated by the decay of single particles with the size of 11 nm. In the intermediate time range, the correlation function can only be fitted by the decays from both the single nanocrystals (around 10 nm) and the superlattices (around 270 nm). Only after 8 h does the size corresponding to  $\tau_{C_1}$  become slightly smaller than the single superlattice size. This was caused by a fitting algorithm error when the contribution from this decay term became very small. The fitting correlation times and the corresponding particle diameters are listed in Table 2. The appearance of both decays in the correlation function rather than a continuous shifting of a single decay function indicates that the dissolution of the superlattices does not occur through continual shrinkage of the average single superlattice size. Instead, the average NCS size remained fairly constant while their numbers decreased. This implies that the NCS fall apart all at once instead of continuously getting smaller. Whether this implies this particular size is a local minimum in stability will remain to be determined with future experimentation. Also included in Table 2 is an extra

**TABLE 2: Fitting Results of DLS Correlation Function Measurement of the NCSs Dissociation Process**

time (h)	$\tau_{c1}$ (ms)	$d_1$ (nm)	$\tau_{c2}$ (ms)	$d_2$ (nm)	$\tau_{c3}$ (ms)	$d_3$ ( $\mu$ m)
0			1.48	502		
2.5	0.023	7.9	0.85	289	127	42.9
3	0.042	14	0.83	280	138	46.6
4	0.039	13	0.81	274	117	39.5
5	0.059	19	0.84	283	110	37.1
6	0.054	18	0.83	255	124	41.9
7	0.047	16	0.36	121	61	20.1
8	0.033	11	0.24	80	52	17.6

decay  $\tau_{c3}$  with a very large decay time (110 ms). We believe that this corresponds to some irreversible aggregation caused by the impurity ions or possibly the dissociation of the ligands from the nanocrystal surface. If the same colloid was left at 80 °C for more than 24 h, it decolorized and formed irreversible aggregates at the bottom of the vial. This unpleasant modification of the nanocrystal surface was also responsible for the slight decrease of the surface plasmon peak at 530 nm as the colloid was heated. As a final note, the DLS study of the NCS dissolution took a much longer time (several hours) as compared with the UV-vis study (10 min). This is because DLS probes the large size particles much more efficiently than the small size particles due to their strong scattering intensity (scattering proportional to volume squared), while for UV-vis spectroscopy the absorption is at most proportional to the volume and perhaps only proportional to the free surface (volume to the two-thirds power). As a result, as long as there are still a few superlattices left in the colloid, the correlation function would still reflect their presence and its change would be relatively slow.

To summarize, we have synthesized nanocrystal superlattices (NCSs) directly in a gold colloid solution through ligating the gold nanocrystal surface with dodecanethiol. DLS proved the existence of tertiary structures in the colloid, namely, single nanocrystals, nanocrystal superlattices, and superlattice aggregates. A rough phase diagram between single nanocrystals and superlattices was given by studying the formation of superlattice structures in colloids with different concentrations and temperatures. Dissolution of the superlattices after raising the temperature across the phase boundary was studied by both DLS and UV-vis spectroscopy.

**Acknowledgment.** This work received partial support from National Science Foundation Grant CTS9709764. We acknowledge the help from the Kansas State University Biology Research Microscope and Image Processing Facility, which has been supported in part by the Kansas NSF EPSCoR Program, by the Kansas NASA EPSCoR Program, by University resources, and by the Kansas Agricultural Experiment Station.

## References and Notes

- (1) Alivisatos, A. P. *Science* **1996**, *271*, 933; Shi, J.; Gider, S.; Babcock, D.; Awschalom, D. D. *Science* **1996**, *271*, 937.
- (2) Weller, H. *Angew. Chem., Int. Ed. Engl.* **1996**, *35*, 1079.
- (3) Collier, C. P.; Vossmeier, T.; Heath, J. R. *Annu. Rev. Phys. Chem.* **1998**, *49*, 371.
- (4) Xia, Y.; Kim, E.; Mrksich, M.; Whitesides, G. M. *Chem. Mater.* **1996**, *8*, 601; Kamar, A.; Whitesides, G. M. *Science* **1994**, *263*, 601.
- (5) Jin, B. Y.; Ketteren, J. B. *Adv. Phys.* **1988**, *38*, 189.
- (6) Murray, C. B.; Kagan, C. R.; Bawendi, M. G. *Science* **1995**, *270*, 1335.
- (7) Yin, J. S.; Wang, Z. L. *Phys. Rev. Lett.* **1997**, *79*, 2570; Yin, J. S.; Wang, Z. L. *J. Phys. Chem. B* **1997**, *101*, 8979.
- (8) Motte, L.; Billoudet, F.; Lacaze, E.; Pileni, M. P. *Adv. Mater.* **1996**, *8*, 1018; Motte, L.; Billoudet, F.; Pileni, M. P. *J. Phys. Chem.* **1995**, *99*, 16425; Motte, L.; Billoudet, F.; Lacaze, E.; Douin, J.; Pileni, M. P. *J. Phys. Chem.* **1997**, *101*, 138.
- (9) Korgel, B. A.; Fitzmaurice, D. *Phys. Rev. Lett.* **1998**, *80*, 3531.
- (10) Korgel, B. A.; Fullam, S.; Connolly, S.; Fitzmaurice, D. *J. Phys. Chem. B* **1998**, *102*, 8379.
- (11) Ohara, P. C.; Leff, D. V.; Heath, J. R.; Gelbart, W. M. *Phys. Rev. Lett.* **1995**, *75*, 3466.
- (12) Andres, R. P.; Bielefeld, J. D.; Henderson, J. I.; James, D. B.; Lolagunta, V. R.; Kubiak, C. P.; Mahoney, W. J.; Osifchin, R. G. *Science* **1996**, *273*, 1690.
- (13) Nagayama, K. *Colloids Surf.* **1996**, *109*, 363.
- (14) Trau, M.; Saville, D. A.; Aksay, I. A. *Science* **1996**, *272*, 706; Trau, M.; Saville, D. A.; Aksay, I. A. *Langmuir* **1997**, *13*, 6375.
- (15) Whetten, R. L.; Khoury, J. T.; Alvarez, M. M.; Murthy, S.; Verma, I.; Wang, Z. L.; Stephens, P. W.; Cleveland, C. L.; Luedtke, W. D.; Landman, U. *Adv. Mater.* **1996**, *8*, 428; Harfenist, S. A.; Wang, Z. L.; Alvarez, M. M.; Verma, I.; Whetten, R. L. *J. Phys. Chem.* **1996**, *100*, 13904; Wang, Z. L.; Harfenist, S. A.; Verma, I.; Whetten, R. L.; Bentley, J.; Evans, N. D.; Alexander, K. B. *Adv. Mater.* **1998**, *10*, 808.
- (16) Cusack, L.; Rizza, R.; Gorelov, A.; Fitzmaurice, D. *Angew. Chem., Int. Ed. Engl.* **1997**, *36*, 848.
- (17) Lin, X. M.; Sorensen, C. M.; Klabunde, K. J. *Chem. Mater.* **1999**, *11*, 198.
- (18) Wilcoxon, J. P.; Williamson, R. L.; Baughman, R. J. *Chem. Phys.* **1993**, *98*, 9933.
- (19) Quinten, M.; Kreibitz, U. *Surf. Sci.* **1986**, *172*, 557.
- (20) Weiner, B. B. *Particle Size Analysis*; Stanley-Wood, N. N., Lines, R. W., Eds.; Royal Society of Chemistry: Cambridge, 1992; pp 173–185.
- (21) Gorden, J. P.; Leite, R. C. C.; More, R. S.; Porto, S. P.; Whinnery, J. R. *J. Appl. Phys. Lett.* **1965**, *36*, 3; Whinnery, J. R.; Miller, D. T.; Dabby, F. *IEEE J. Quantum Electron.* **1967**, *QE-3*, 383; Callen, W. R.; Huth, B. G.; Pantell, R. H. *Appl. Phys. Lett.* **1967**, *11*, 103.
- (22) Lin, X. M.; Wang, G. M.; Sorensen, C. M.; Klabunde, K. J. *Appl. Opt.* **1999**, *38*, 1884.
- (23) Asher, S. A.; Holtz, J.; Liu, L.; Wu, Z. *J. Am. Chem. Soc.* **1994**, *116*, 4997.
- (24) Hunter, R. J. *Introduction to Modern Colloid Science*; Oxford University Press: New York, 1993; p 269.
- (25) Derjaguin, B. V.; Landau, L. *Acta Physiocochem. URSS* **1941**, *10*, 25; Verwey, E. J. W.; Overbeek, J. Th. G. *Theory of Stability of Lyophobic Colloids*; Elsevier: Amsterdam, 1948.
- (26) Israelachvili, J. N. *Intermolecular and Surface Forces*; Academic Press: San Diego, 1992; p 246.